Differences among Monte Carlo codes in the calculations of voxel *S* values for radionuclide targeted therapy and analysis of their impact on absorbed dose evaluations

M. Pacilio[a)]
Department of Medical Physics, Azienda Ospedaliera S. Camillo Forlanini, Piazza Forlanini 1, Rome 00151, Italy

N. Lanconelli and S. Lo Meo
Department of Physics, Alma Mater Studiorum University of Bologna, Viale Berti-Pichat 6/2, Bologna 40127, Italy

M. Betti
Department of Medical Physics, Azienda Ospedaliera S. Camillo Forlanini, Piazza Forlanini 1, Rome 00151, Italy

L. Montani
Department of Medical Physics, Azienda Ospedaliera Sant'Andrea, Via di Grotarossa 1035, Rome 00189, Italy

L. A. Torres Aroche and M. A. Coca Pérez
Department of Medical Physics, Center for Clinical Researches, Calle 34 North 4501, Havana 11300, Cuba

(Received 22 January 2009; revised 2 March 2009; accepted for publication 2 March 2009; published 8 April 2009)

Several updated Monte Carlo (MC) codes are available to perform calculations of voxel *S* values for radionuclide targeted therapy. The aim of this work is to analyze the differences in the calculations obtained by different MC codes and their impact on absorbed dose evaluations performed by voxel dosimetry. Voxel *S* values for monoenergetic sources (electrons and photons) and different radionuclides (^{90}Y, ^{131}I, and ^{188}Re) were calculated. Simulations were performed in soft tissue. Three general-purpose MC codes were employed for simulating radiation transport: MCNP4C, EGSnrc, and GEANT4. The data published by the MIRD Committee in Pamphlet No. 17, obtained with the EGS4 MC code, were also included in the comparisons. The impact of the differences (in terms of voxel *S* values) among the MC codes was also studied by convolution calculations of the absorbed dose in a volume of interest. For uniform activity distribution of a given radionuclide, dose calculations were performed on spherical and elliptical volumes, varying the mass from 1 to 500 g. For simulations with monochromatic sources, differences for self-irradiation voxel *S* values were mostly confined within 10% for both photons and electrons, but with electron energy less than 500 keV, the voxel *S* values referred to the first neighbor voxels showed large differences (up to 130%, with respect to EGSnrc) among the updated MC codes. For radionuclide simulations, noticeable differences arose in voxel *S* values, especially in the bremsstrahlung tails, or when a high contribution from electrons with energy of less than 500 keV is involved. In particular, for ^{90}Y the updated codes showed a remarkable divergence in the bremsstrahlung region (up to about 90% in terms of voxel *S* values) with respect to the EGS4 code. Further, variations were observed up to about 30%, for small source-target voxel distances, when low-energy electrons cover an important part of the emission spectrum of the radionuclide (in our case, for ^{131}I). For ^{90}Y and ^{188}Re, the differences among the various codes have a negligible impact (within few percents) on convolution calculations of the absorbed dose; thus either one of the MC programs is suitable to produce voxel *S* values for radionuclide targeted therapy dosimetry. However, if a low-energy beta-emitting radionuclide is considered, these differences can affect also dose depositions at small source-target voxel distances, leading to more conspicuous variations (about 9% for ^{131}I) when calculating the absorbed dose in the volume of interest. © *2009 American Association of Physicists in Medicine*. [DOI: 10.1118/1.3103401]

Key words: Monte Carlo, targeted radiotherapy, MIRD

I. INTRODUCTION

Radionuclide targeted therapy is a current clinical and research field that has shown a rapid expansion in the past few years. Optimized imaging modalities (PET/CT or SPECT/CT) and new tracers have increased the possibilities for therapeutic applications. Patient-specific internal dosimetry remains a critical issue for calculating the activity delivering a proper radiation dose to the tumor, while protecting critical

organs. The accurate determination of absorbed dose in tissues is essential for treatment planning and establishing the dose-effect relationships in terms both of tumor control and normal tissue complications. In most clinical trials and therapeutic applications, the basic formalism of the Medical Internal Dose Committee (MIRD) of the Society of Nuclear Medicine has been used.[1] This formalism, originally developed for internal dosimetry in diagnostic nuclear medicine, is based on the use of radionuclide specific *S* values defined as the mean absorbed dose to a target organ per radioactive decay in a source organ. Biokinetics are assessed by quantitative imaging techniques, for which accurate guidelines have been established.[2] The use of standard anatomic models and *S* values at the organ level is the major limitation of this approach. Even if "mass adjustments" of the organ *S* values can be performed with morphologic imaging (e.g., CT acquisition), the use of *S* values at the organ level intrinsically implies the assumption of uniform activity distribution in the organ. Dosimetric results can be assessed only in terms of mean absorbed dose to the organ; moreover, tumor dosimetry is not included in the model. This method is far from the treatment planning procedure commonly used in other radiation therapy modalities, in which a "figure of merit" for the appropriateness of the treatment can be obtained [i.e., the dose volume histograms (DVHs) for tumor and critical organs]. However, there is nothing intrinsic in the MIRD schema that precludes its extension to take into account nonuniform source distributions. With this aim, MIRD Pamphlet No. 17 has introduced voxel dosimetry to allow dosimetric calculations at the voxel level.[3] Extensive tabulations of voxel *S* values were calculated for many radionuclides with the EGS4 Monte Carlo (MC) code, for two voxel dimensions (3 and 6 mm). Applying the voxel dosimetry method on coregistered SPECT\CT or PET\CT images, and with a segmentation tool to define organs and tumors, it is possible to calculate isodose curves and DVHs for each volume of interest. This approach can be considered as real treatment planning procedure, at least for anatomic regions, which are characterized by uniform density tissue. As the voxel dimensions may vary between imaging systems, each institution should perform MC calculations of *S* values for the voxel size of interest.[4] Nowadays, several updated MC codes are available to simulate radiation transport. Some efficient MC programs were specifically developed for voxel-based dosimetry in radiotherapy and brachytherapy treatment planning.[5–8]

The aim of this work is to compare the calculations of energy deposition at the voxel level performed by different MC codes for radionuclide targeted therapy dosimetry. Other studies have shown that noticeable variations can arise when using different MC programs.[9–11] In this paper, three general-purpose MC codes have been used for simulating radiation transport: MCNP4C, EGSnrc, and GEANT4. MCNP4C code is the extended version of the originally developed Monte Carlo *N*-particle transport code (MCNP). EGSnrc is the latest version in the family of EGS codes, and it was here employed by means of the DOSXYZnrc program. GEANT4 is a general-purpose toolkit initially developed for high-energy physics and today used for a broad range of applications.

Voxel *S* values were calculated for monoenergetic source of electrons and photons and also for three different radionuclides: ^{90}Y, ^{131}I, and ^{188}Re. For comparison purposes with the results of MIRD Pamphlet No. 17, the calculations are referred to 3 and 6 mm voxel size, and radiation transport was simulated in soft tissue, having composition defined by Cristy and Eckerman.[12] To study the impact of the differences in voxel *S* values, a JAVA software program was developed to perform convolution calculations of absorbed dose to spherical and ellipsoidal structures. At this stage, a uniform activity distribution of the radionuclide was assumed in the spherical or ellipsoidal volume, so the associated *S* factor for self-irradiation was calculated, for different tabulations of voxel *S* values as input, by varying also the mass of the volume of interest in a wide range.

II. METHODS

II.A. Monte Carlo codes

MCNP is a general-purpose, continuous energy, generalized geometry, time dependent, coupled neutron/photon/electron MC code. The MCNP4C code[13] is the extended version of the originally developed MCNP code to treat also electron transport, as well as neutron and photon transport, implementing the same algorithms as those of the ITS, Version 3.0. The electron physics enhancements, including changes in the density-effect calculation for collision stopping power, radiative stopping power, calculations of bremsstrahlung spectra and angular distributions, and hard collision events, constitute the most important improvements of this code.[14]

The EGS (electron-gamma-shower) system is a general purpose package for the Monte Carlo simulation of the coupled transport of electrons and photons in an arbitrary geometry for particles with energies above a few keV up to several hundreds of GeV. The EGSnrc MC code implements significant improvements in the physics of radiation transport[15] with respect to EGS4. For instance, the inclusion of relativistic spin effects in elastic scattering cross sections for electrons and the simulation of atomic relaxations after Compton and photoelectric events, together with improved algorithms of electron transport and multiple scattering, increase notably the accuracy of the calculations, especially at low energies. DOSXYZnrc is an EGSnrc-based code for calculating dose distributions in a Cartesian voxel volume: The energy deposition is scored in the designated voxels.[16]

GEANT4 is a general-purpose toolkit that simulates the transport of several particle types in a wide range of energies.[17] It was originally developed for simulating high-energy physics experiments, but nowadays it is also used in various areas of application, including medical physics. GEANT4 allows the simulation of a comprehensive set of physics effects, such as hadronic, electromagnetic, and optical processes. In the last releases, the user can simulate electromagnetic interactions down to energies smaller than 1 keV. For the electromagnetic processes, the user can also

choose among several *Physics lists* (e.g., standard, Penelope, low-energy), which implement different models of radiation transport and cross-section databases for the various effects.[18]

II.B. Simulations

Simulations with MCNP were carried out with the newest electron data library *EL03*, which is the default library for electron transport in MCNP, Version 4C. The database also includes the atomic data of Carlson used in the density-effect calculation. The EL03 evaluation is derived from the ITS, Version 3.0, code system.[19] Also, the electron transport was made with the ITS-style energy indexing algorithm instead of the default MCNP-style energy indexing algorithm. Simulations with DOSXYZnrc code were implemented by activating all the most advanced options available, such as the *electron impact ionization, bound Compton scattering, photoelectron angular sampling, Rayleigh scattering, and atomic relaxations.* In addition, some comparisons were made by using both the default bremsstrahlung cross-section database and that updated by NIST, but no appreciable differences in the results were found. In the following, data obtained by using the NIST database will be presented. Simulations with GEANT4 have been performed with the *standard EM* package, consisting of the following effects: *Photoelectric effect*, Compton scattering, and *gamma conversion* for the transport of photons and *multiple scattering*, *ionization*, and *bremsstrahlung* for the electrons. Some comparisons with the Penelope libraries available with GEANT4 were also performed without noting substantial differences. In the following, all the results shown are obtained with the standard EM package.

The input parameters for the MC simulations, in terms of geometry and composition of source, surrounding medium and scoring regions, were chosen in order to perform direct comparisons with the MIRD data.[3] Electron and photon transports were simulated in a homogeneous medium of soft tissue, having the elemental composition and physical density defined by Cristy and Eckerman.[12] Energy was scored in grids of cubic voxels, having a voxel size of 3 mm, or 6 mm, with the sources uniformly dispersed in a voxel irradiating isotropically the surrounding ones. The centroid of the source voxel was assumed as the origin of the Cartesian system. All simulations have been carried out without using variance reduction techniques, with 2.5×10^7 starting particles and a cutoff energy of 1 keV. The energy scored in each voxel has been converted in average dose to the target voxel per unit of cumulated activity (mGy MBq^{-1} s^{-1}) and associated with the target position in the Cartesian grid. The data comparisons have been represented by reporting the voxel S value as a function of the distance between source voxel and target voxel, including also 3D diagonal distances.

II.C. Source energy spectra

Simulations with monoenergetic source of electrons and photons were performed, varying the energy in the range of 0.1–1.8 MeV for photons and 0.1–10 MeV for electrons. In this case, S values are referred to the 3 mm voxel and have been reported just for the voxel where the source is located (self-irradiation) and for its two closest voxels. Moreover, ^{90}Y, ^{131}I, and ^{188}Re sources were simulated. For radionuclides, S values were reported for all the voxels with a distance from the source voxel of up to 20 mm. Nuclear decay data have been obtained from Brookhaven National Laboratory (http://www.nndc.bnl.gov/nudat2/) and Lawrence Berkeley National Laboratory (http://ie.lbl.gov/toi/index.asp). In Fig. 1, the beta spectra of the radionuclides considered in this study have been reported. Beta emissions were simulated as a discrete spectrum of monoenergetic electrons.

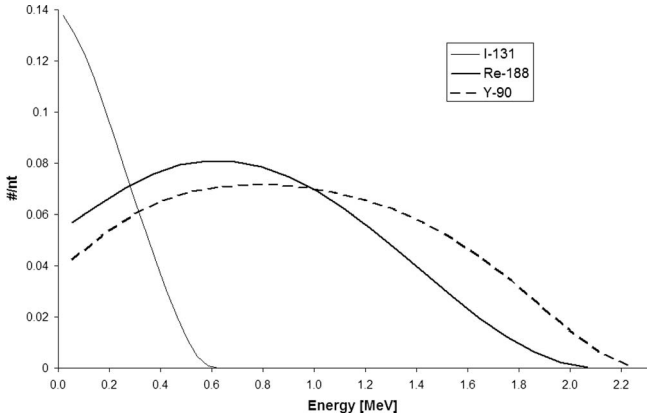

FIG. 1. Beta spectra (frequency of beta emission versus energy) for ^{131}I, ^{188}Re, and ^{90}Y.

II.D. Absorbed dose calculations

To assess the dosimetric impact of the differences in voxel S values among several MC codes, the absorbed dose to spherical and elliptical volumes of soft tissue was calculated by means of the voxel S value tabulations obtained from the MC codes. To perform dosimetric convolution calculations by the MIRD method applied at the voxel level,[3] a JAVA software program (CALDOSE, calculations of dose on spheres and ellipsoids) was developed. The inputs of the software are voxel S values tabulated with respect to the position indices (i,j,k), voxel size, sphere radius or ellipsoid axes, and cumulated activity contained in the voxels. Voxel S-value tables are loaded as a text file, whereas the other parameters are entered by interactive windows. The output is the dose absorbed per unit of cumulated activity (mGy MBq^{-1} s^{-1}), i.e., the S factor for self-irradiation associated with the sphere/ellipsoid mass. As the voxel S values in the MIRD Pamphlet No. 17 are listed with position indices up to (5,5,5), the voxel S-value tabulations calculated here were truncated to these (i,j,k) values for convolution calculations. Only rotational ellipsoids have been considered, with a major axis fourfold the minor axis, and only uniform distributions of the radionuclides have been assumed. The volume of spheres and ellipsoids has been varied, and the data comparison has been represented reporting the percent differences in the absorbed dose with respect to the value obtained by published voxel S values,[3] as a function of the sphere/ellipsoid

mass. For ^{188}Re, voxel *S* values are not available in the MIRD publication, so the comparison was represented considering the results from EGSnrc as reference values.

III. RESULTS AND DISCUSSION

III.A. Uncertainties estimation

The statistical uncertainties associated with the voxel *S* values are dependent on the voxel size and the source-target voxel distance, as well as the number, energy, and type (electrons or photons) of starting particles. For instance, the self-irradiation *S* values for a 3 mm voxel size had the following statistical uncertainties: 0.01%–0.02% for the radionuclide beta spectra, 0.04%–0.3% for the monoenergetic electrons, 0.2%–0.5% for the radionuclide photon emissions, and 0.2%–0.3% for the monoenergetic photons. For a given voxel size, the statistical uncertainty increased with the source-target voxel distance due to the lowering of the interaction number in the scoring volume. For instance, for the 3 mm voxel size, the *S* values for the target voxel with position indices (5,5,5) had the following statistical uncertainties: 21% for both ^{90}Y and ^{188}Re beta spectra, 46% for ^{131}I beta spectra, whereas for photon emission 4% for ^{188}Re and ^{131}I. The statistical uncertainties have been reported in the figures as error bars. However, in the majority of the cases simulated in this work the statistical error is small, and the associated error bars are barely visible on the plots because they are confined within the size of the markers. When the differences with respect to EGS4 are considered, it is not possible to assess the uncertainties since the uncertainties associated to EGS4 data are unknown (MIRD Pamphlet No. 17 provides neither the uncertainties, nor the number of simulated histories).

III.B. Monochromatic electron and photon sources

Monoenergetic emissions of electrons and photons have been simulated in a wide energy range. In Fig. 2(a), the results of *S* value for self irradiation, referred to a voxel size of 3 mm, have been reported as a function of the electron energy. For EGSnrc, the differences (calculated with respect to MCNP4C) yield about 4% at 0.6 MeV, to 1.6% at 1.8 MeV and 1.4% at 2.1 MeV, remaining constant (about 1%) at higher energies. For GEANT4, differences yield about −3.3% at 1.2 MeV and remain between −3.5% and −2.5% at higher energies. Figure 2(b) reports the results for photons, analogous to Fig. 2(a). For EGSnrc, the differences are within 6% up to 0.4 MeV and yield up to 7% for higher energies. For GEANT4, the differences are analogous, but with the opposite sign. So, in the energy range typical for the nuclear irradiative emissions of the radionuclides in this study (roughly, up to 0.4 MeV for gamma and 2.2 MeV for beta emissions), different MC codes yield differences in a few percent for the self-irradiation voxel *S* values.

The results concerning the energy deposited in the first neighbor voxels (which are also expected to give consistent contributions in terms of absorbed dose) have also been reported. Figures 3(a) and 3(b) show the percent differences

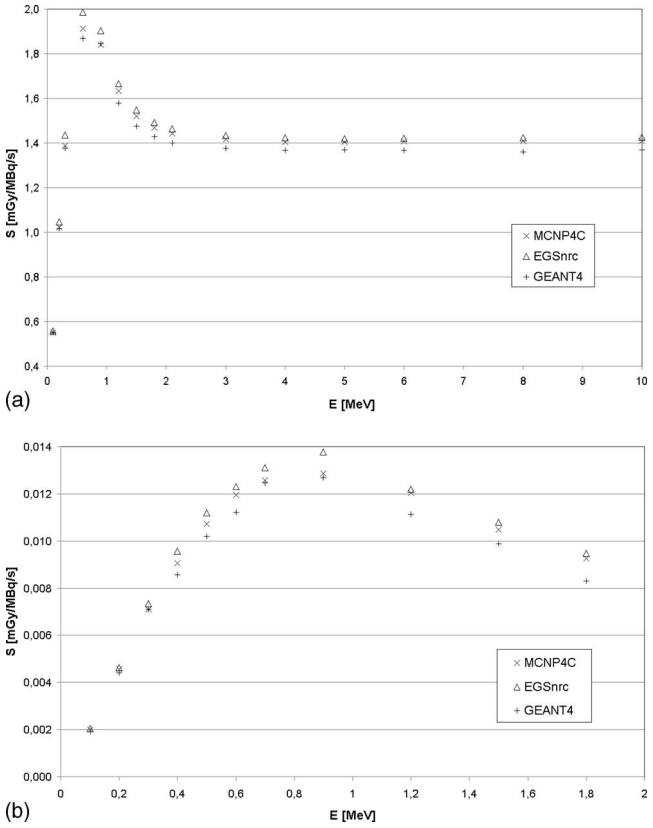

FIG. 2. Self-irradiation voxel *S* values, for a 3 mm voxel size, calculated with monochromatic electron (a) and photon (b) sources. Errors are within the symbol size.

with respect to EGSnrc results for 3 mm voxels with monochromatic electron and photon sources, respectively. Two neighbor voxels were considered: One at a distance of 3 mm from the central one (named 001) and one at a distance of 4.2 mm from the central one (named 011). The results reported in Fig. 2 [voxel with position indices (0,0,0)] have been considered also in Fig. 3. It is worth noting that the differences for electron self-irradiation (dataset e-000) and for photons *S* values (datasets ph-000, ph-001, and ph-011) are mostly confined within 10%. While the differences for electron *S* values referred to the neighbor voxels are much bigger, at low energies, differences for the datasets e-001 and e-011 reach 70% and 130%, respectively. This should be related to the different models for electrons transport and agrees with what other authors observed in similar conditions for GEANT4 and EGSnrc.[18] They found differences of a few percent in the dose deposition of photons in a water phantom, and a larger difference for low-energy electrons. In addition, it is worth mentioning that, as observed also by Poon and Verhaegen for 1 MeV electrons,[18] the dose calculated by GEANT4 is smaller for electrons at shallow depths (up to about 2 mm), whereas it is larger for deeper positions (more than 2 mm). A similar result was achieved for MCNP by Wang and Li,[9] in a comparison among EGS4, EGSnrc, and MCNP. This effect is much more evident for electrons with lower energies, as can be seen in Fig. 3(a). It could lead to differences in dose calculations between the various codes, especially when low-

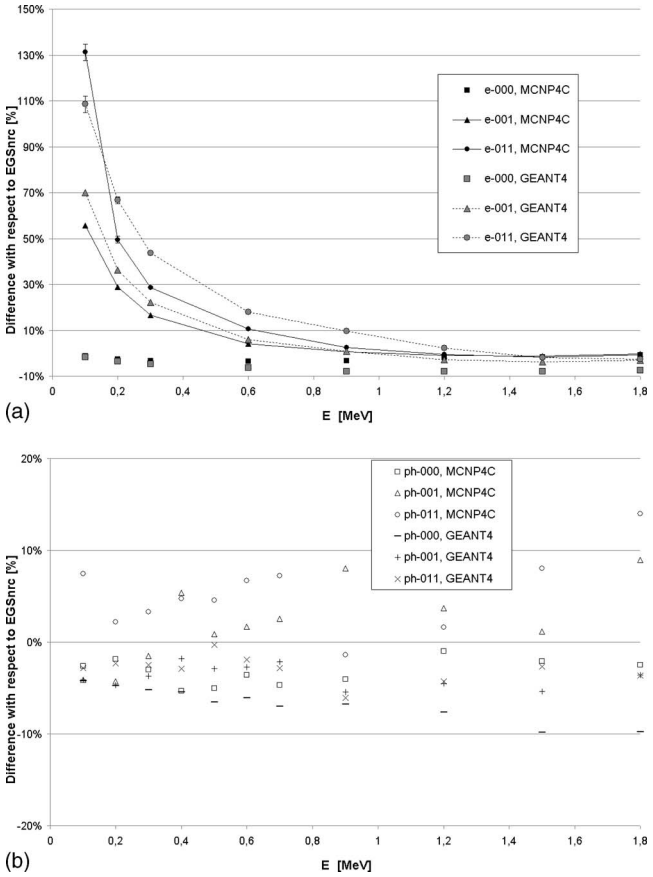

FIG. 3. Percent differences in MCNP4C and GEANT4 *S* values calculated for the monochromatic electron (a) and photon (b) sources with respect to EGSnrc data. Differences are shown for the self-irradiation voxel (000), and two voxels located at distances of 3 mm (001) and 4.2 mm (011) from the central one. Error bar is shown when they exceed the symbol size [only for low-energy electrons at 4.2 mm distance (011)].

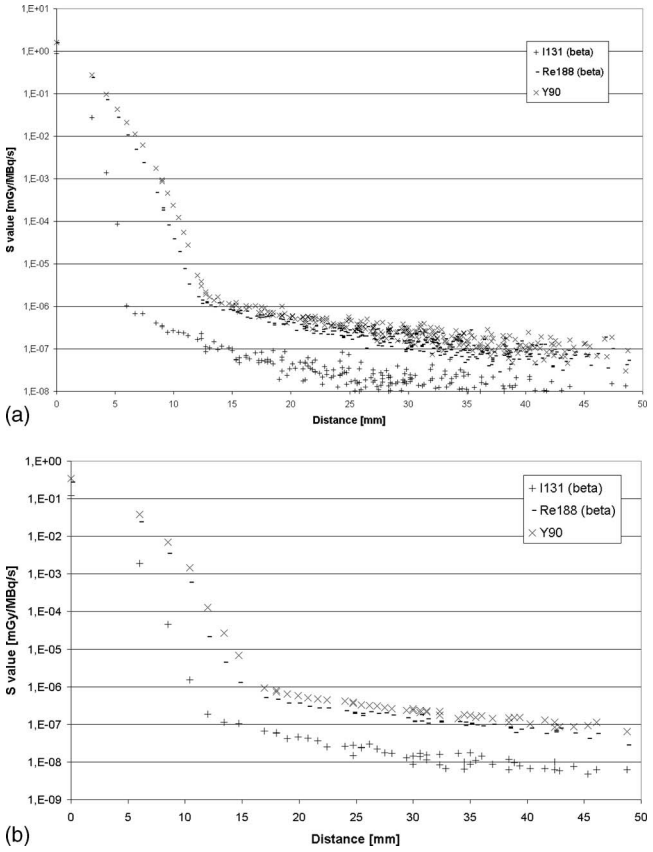

FIG. 4. Voxel *S* values due to beta emissions, for the radionuclides in this study, as a function of the source voxel-target voxel distance for a voxel size of 3 mm (a) and 6 mm (b). The data were obtained with the MCNP4C MC code.

energy electrons cover an important part of the emission spectrum of the radionuclide. It should be mentioned that the voxel *S* values from the first neighbor voxels decrease strongly with energy, down to values two to three orders of magnitude lower than self-irradiation ones, for energy less than 500 keV, limiting the overall impact of these differences for clinical dosimetry.

III.C. Radionuclides

In Fig. 4 a comparison among the voxel *S* values due to beta emissions of the radionuclides in this study, as a function of the source-target voxel distance, is reported for 3 mm [Fig. 4(a)] and 6 mm [Fig. 4(b)] voxel size. The data have been obtained with the MCNP4C code. The curves have similar, regular trends, dependent on the beta emission spectra. An abrupt change in slope is present at distances where the beta contribution becomes negligible with respect to the bremsstrahlung contribution. Two of the three considered radionuclides (^{90}Y and ^{188}Re) have comparable beta emission spectra with a maximum energy of about 2 MeV, whereas ^{131}I presents a spectrum positioned at lower energies (maximum energy of about 800 keV). This is reflected in the very similar behavior of the first two radionuclides in Fig. 4, while ^{131}I, as a result of its lower energy, is characterized by a dose deposition localized at smaller distances. For the 3 mm voxel, the statistical uncertainty of the results increases with distance, evidencing a greater statistical uncertainty in the bremsstrahlung region. The calculations have also been performed by the other MC codes. The total voxel *S* values, including both beta and gamma emission contributions, have been calculated and reported in the following figures.

The comparisons among the results obtained with the MC codes employed here, and those from MIRD Pamphlet No. 17 (calculated with EGS4) are reported in Figs. 5–10. In Fig. 5, the data referred to ^{90}Y are represented, in terms of voxel *S* values [Fig. 5(a)] and percent differences with respect to the EGS4 data [Fig. 5(b)[, for a voxel size of 3 mm. Analogously, in Fig. 6, the ^{90}Y voxel *S* values [Fig. 6(a)] and associated percent differences [Fig. 6(b)] are reported for a voxel size of 6 mm. Consistent differences are visible for both voxel sizes at large distances, around the larger curve slope change. For 3 mm voxel, the differences range from −50% to −90% with the distance ranging from 10 to 13 mm, remaining constant at about −90% up to a distance of about 17 mm. For 6 mm voxel, the differences range from −50% to −90% with the distance ranging from 10 to 17 mm. It can be noticed that the large divergences in the

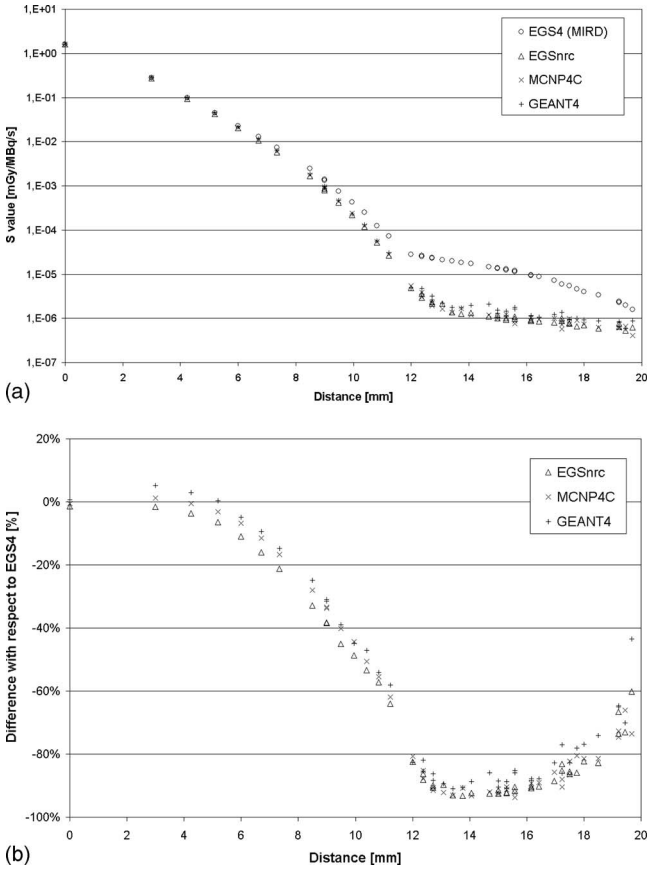

FIG. 5. Voxel *S* values for ^{90}Y, for a voxel size of 3 mm, as a function of the source-target voxel distance, obtained by several MC codes (a). Errors are within the symbol size. The percent differences with respect to the EGS4 values are also reported (b).

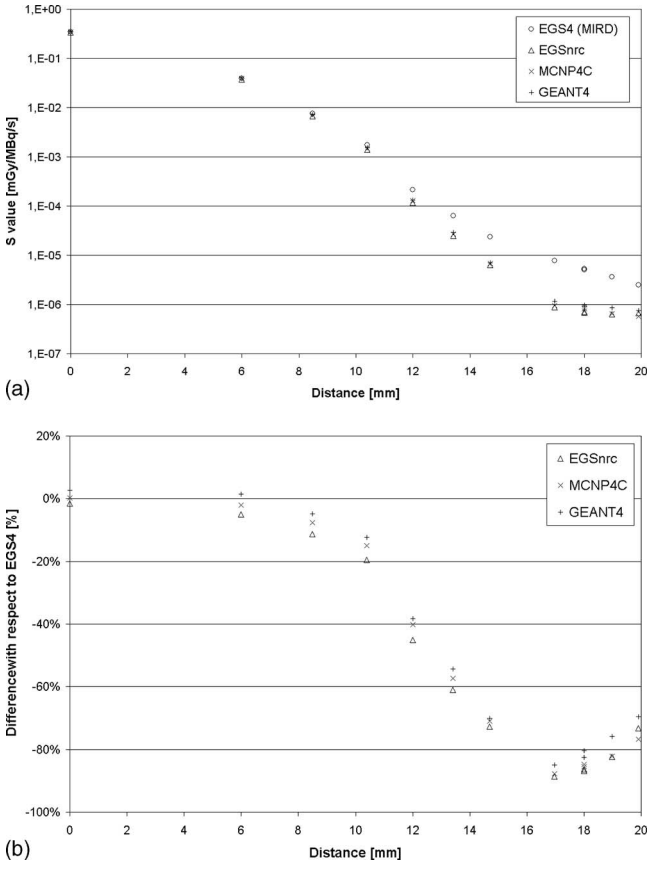

FIG. 6. Voxel *S* values for ^{90}Y, for a voxel size of 6 mm, as a function of the source-target voxel distance, obtained by several MC codes (a). Errors are within the symbol size. The percent differences with respect to the EGS4 values are also reported (b).

bremsstrahlung region, with respect to MIRD data, are very similar for all the three updated MC codes. These discrepancies may be due to the radiation transport methods used in the older EGS4 program used for MIRD calculations. In particular, as already noted by Wang and Li,[9] the differences may be partially attributed to the different models for electron transport and multiple scattering theories. Further, some differences can also arise from the different cross-section libraries adopted by the various codes. A more complete description of the various models for particle transport available with the different codes can be found in some papers cited in the reference section.[9,10,18,20]

In Figs. 7 and 8 the same comparisons have been reported for ^{131}I. From Fig. 7 (voxel size of 3 mm), differences are evidenced at short distances. At about 4 mm, the difference reaches −31% for EGSnrc, −26% for MCNP4C, and −24% for GEANT4. At larger distances, differences are scattered between −20% and 20% for most values. Here the fluctuations are pretty large because of the low-energy spectrum of ^{131}I, which causes a poorer statistics at large distances. For a voxel size of 6 mm (Fig. 8), the trend is analogous, but the differences are averaged on a larger volume. So, for EGSnrc the maximum difference reaches −22% at 6 mm, whereas most values are between −10% and 3% at distances larger than 10 mm. Even if the variations are smaller than those observed for ^{90}Y, they can affect more significantly dose calculations, as they occur at smaller distances.

In Figs. 9 and 10, the data regarding ^{188}Re are reported. In this case, comparison with the MIRD results is not possible, as the calculations have not been performed for this radionuclide. Thus, the differences have been calculated with respect to the EGSnrc results. For the 3 mm voxel size (Fig. 9), the differences in GEANT4 start to increase with distance, reaching a value of about 20% at about 9 mm. After, the differences drop with distance and remain between ±10% at distances greater than 12 mm. On the other hand, MCNP4C values are similar to the EGSnrc results (differences within 3%) up to a distance of about 7 mm. Then, differences increase abruptly with distance, reaching a mean value of about 70% at distances greater than 12 mm. For the 6 mm voxel size (Fig. 10), the data are analogous even if the differences are slightly mitigated due to the averaging on the bigger voxel volume.

III.D. Absorbed dose calculation

In Fig. 11, the comparison among the MC codes, in terms of absorbed dose calculations per unit of cumulated activity, is shown for ^{90}Y. The difference between the dose calculation obtained by the voxel *S* values of a given MC code, with

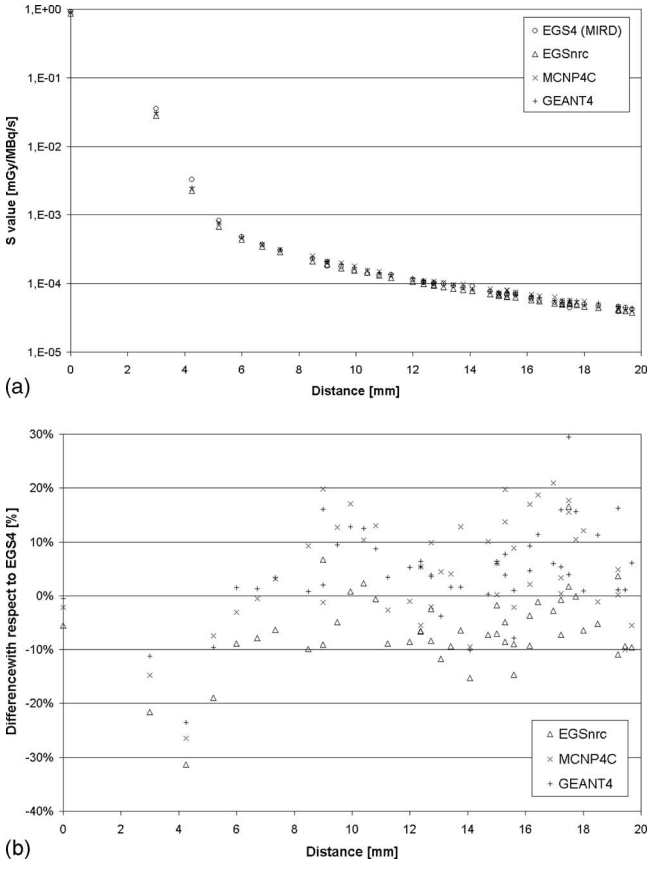

FIG. 7. Voxel *S* values for ^{131}I, for a voxel size of 3 mm, as a function of the source-target voxel distance, obtained by several MC codes (a). Errors are within the symbol size. The percent differences with respect to the EGS4 values are also reported (b).

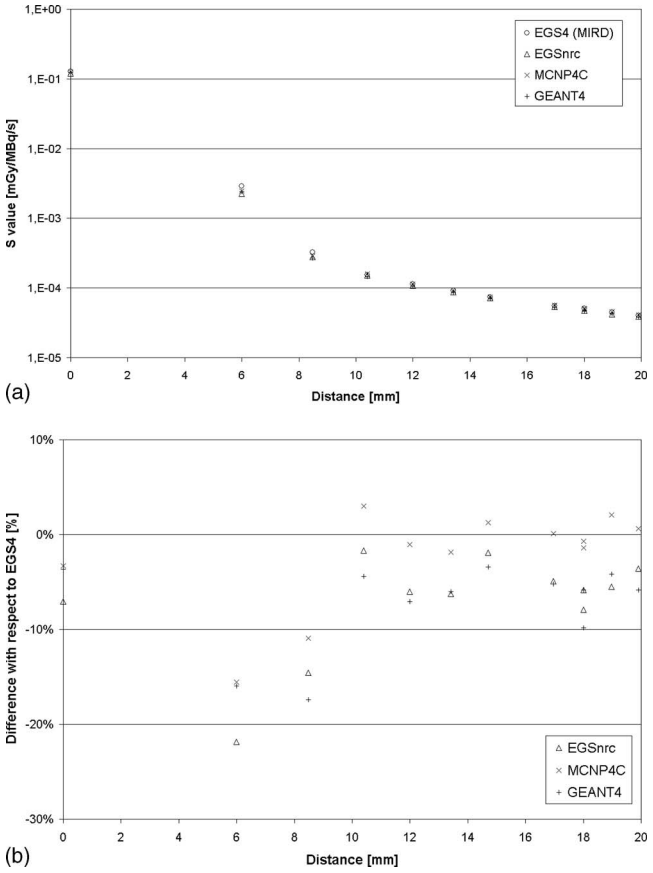

FIG. 8. Voxel *S* values for ^{131}I, for a voxel size of 6 mm, as a function of the source-target voxel distance, obtained by several MC codes (a). Errors are within the symbol size. The percent differences with respect to the EGS4 values are also reported (b).

respect to the same calculation performed by the published *S* value tabulation,[3] has been represented with volume-of-interest mass (sphere or ellipsoid), up to 100 g. The data have been obtained with the *S* values referred to the 3 mm voxel size. Despite the big differences observed at large distances in the voxel *S*-value comparison (see Fig. 5), the impact on the absorbed dose is limited: Indeed, considering all the MC codes, the differences reach a constant value between −4% and 2%. Moreover, the results for spheres and ellipsoids are in substantial agreement for each code, up to masses of 500 g.

Figure 12 reports the same comparison for ^{131}I, and differences with respect to EGS4 are more evident. Dose calculations evidence that the differences reach a value of about −9% for EGSnrc, −5% for MCNP4C, and −3% for GEANT4, at a mass of 20 g, remaining constant for higher masses. Also in this case, the comparison between ellipsoidal and spherical masses shows a good agreement, and the data trend is constant up to masses of 500 g. The larger difference observed, with respect to that obtained with ^{90}Y, is basically due to the higher contribution of low-energy electrons to the ^{131}I beta spectrum. Indeed, the beta spectrum of this radionuclide has a maximum energy of about 800 keV and, as already noted in Fig. 3, this is the range where the largest variations in the transport of electrons among the various codes can be observed.

In Fig. 13, data for ^{188}Re are given. In this case, dose differences have been assessed with respect to EGSnrc dose calculations. The percent differences are negligible for both codes. In particular, MCNP4C, thanks to the great similarity with *S* values estimated by EGSnrc at small distances, reaches a maximum difference of about 1%. On the other hand, GEANT4 shows slightly larger differences, still limited to less than 3%. A substantial agreement between spherical and ellipsoidal masses is evidenced, and also in this case, differences reach a plateau value which remains constant up to masses of 500 g.

In this study, differences among several MC codes have been evidenced for simulations with monochromatic sources, above all in simulating the transport of low-energy electrons. In particular, these differences are larger for the EGSnrc code. Also, voxel *S*-value differences among several MC codes have been reported for all the radionuclides considered here. On the other hand, the influence of voxel *S*-value differences on dose calculations is strongly dependent also on the value at which the difference is referred. At large distances from the source voxel, the voxel *S* value is several order of magnitude lower, so its relative contribution to the absorbed dose is negligible, and it was confirmed here by

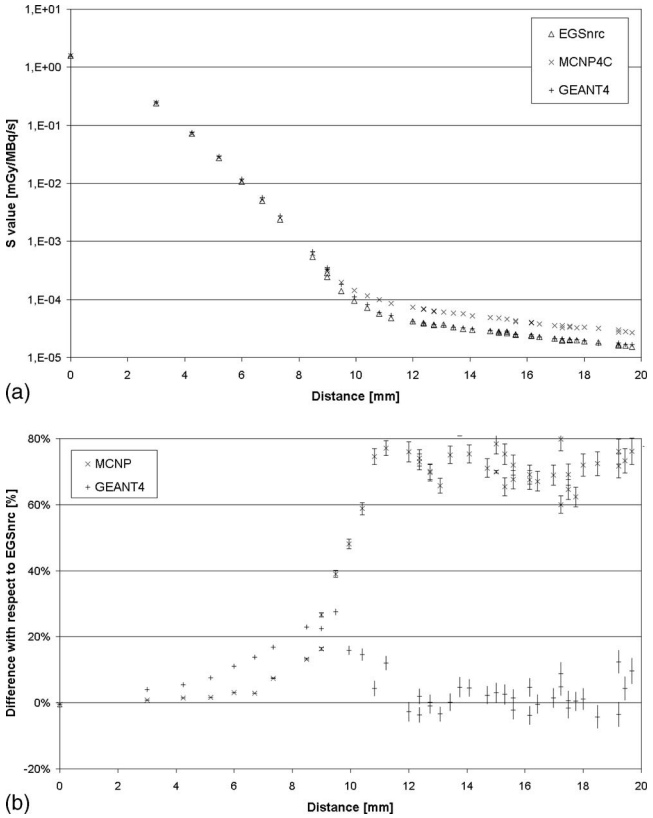

FIG. 9. Voxel *S* values for ^{188}Re, for a voxel size of 3 mm, as a function of the source-target voxel distance, obtained by several MC codes (a). Errors are within the symbol size. The percent differences (b) have been calculated with respect to the EGSnrc values. Error bars have been reported.

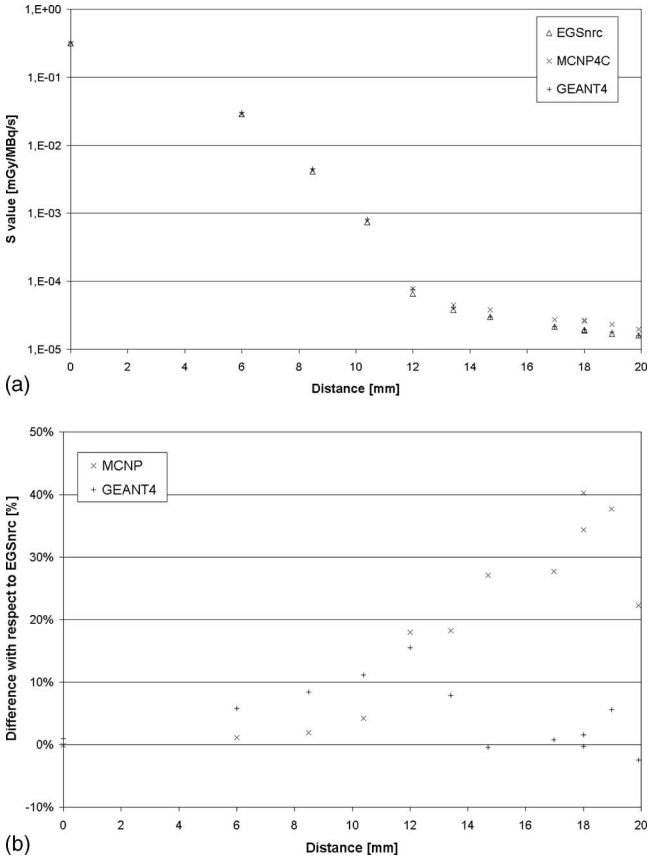

FIG. 10. Voxel *S* values for ^{188}Re, for a voxel size of 6 mm, as a function of the source-target voxel distance, obtained by several MC codes (a). The percent differences (b) have been calculated with respect to the EGSnrc values. For both plots, errors are within the symbol size.

dose calculations referred to ^{90}Y and ^{188}Re. More consistent differences in the absorbed dose have been evidenced for ^{131}I. Indeed, the lower energy contributions to the beta spectrum, together with the differences in modeling low-energy electron transport among the MC codes, generate stronger differences in the voxel *S* values referred to first neighbor voxels, affecting more significantly the dose calculations, even though the overall maximum difference on the absorbed dose is still modest (9%). In radionuclide targeted therapy, the level of accuracy of the patient-individualized dosimetry is a crucial problem, and frequently, the assessed uncertainty in absorbed dose calculations is pretty large (at least $\pm$50%), depending on the method used for dosimetry evaluations.[21,22] Nevertheless, if it is possible to accomplish an accurate optimization of the several phases in the dosimetric study (data acquisition, image quantification, data processing, and evaluation of the individual organ volumes), then it could be possible to reduce the total uncertainty of the individual dose estimate to about $\pm$10%–20%.[2,23] In this case, the maximum difference reported in the present study for a low-energy beta emitter could become noteworthy.

IV. CONCLUSION

This paper presents an intercomparison among published data for voxel *S* values and the results obtained by three updated MC codes. Both voxel *S* values and a convolution

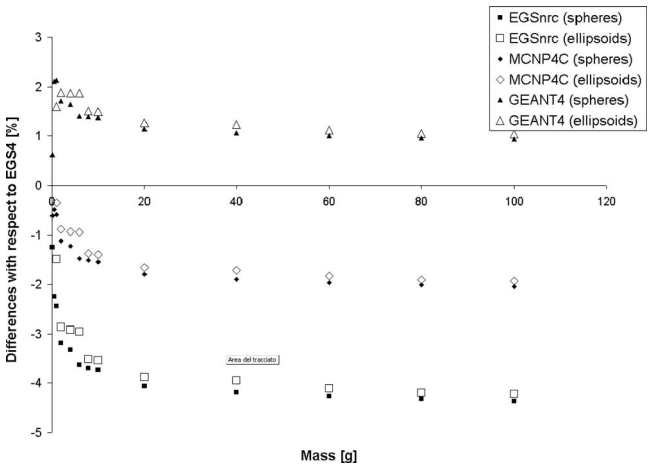

FIG. 11. Comparison of absorbed dose calculation for unit of cumulated activity, among several MC codes, for ^{90}Y. Calculations are referred to the *S*-value tabulations for the 3 mm voxel size. The data are reported in terms of the percent differences with respect to the calculations obtained by the EGS4 voxel *S* values (the published tabulations) for both spherical and ellipsoidal masses.

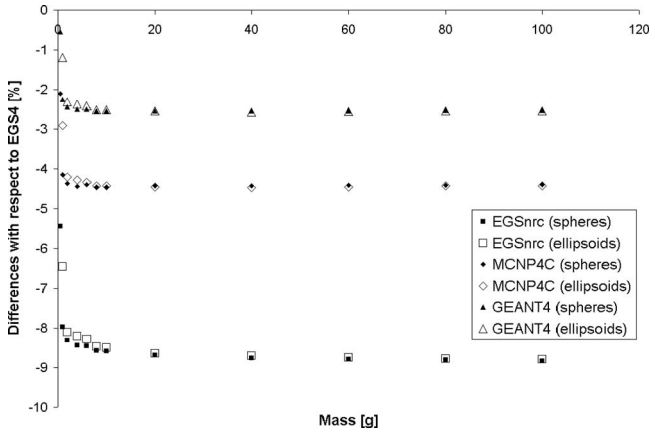

FIG. 12. Comparison of absorbed dose calculation for unit of cumulated activity, among several MC codes, for ^{131}I. Calculations are referred to the *S*-value tabulations for the 3 mm voxel size. The data are reported in terms of the percent differences with respect to the calculations obtained by the EGS4 voxel *S* values (the published tabulations) for both spherical and ellipsoidal masses.

estimate of the absorbed dose for spherical and ellipsoidal masses were calculated. Noticeable differences arise in voxel *S* values, especially in the bremsstrahlung tails for radionuclide simulations, or in the presence of electrons with energy less than 500 keV. In particular, the updated codes show a remarkable divergence in the bremsstrahlung range (up to about 90% in term of voxel *S* values) with respect to previous MC codes. Nevertheless, these variations occur at large distances; thus, they have a little impact when considering the convolution calculation of the absorbed dose for objects with a certain volume. Our results suggest that in most cases the differences among the various codes affect poorly (within a few percent) convolution calculations of the absorbed dose, thus either one of the MC programs is suitable to perform this kind of dose estimations. However for low-energy electrons, variations in terms of voxel *S* values can rise notably. So, if a low-energy beta-emitting radionuclide is considered,

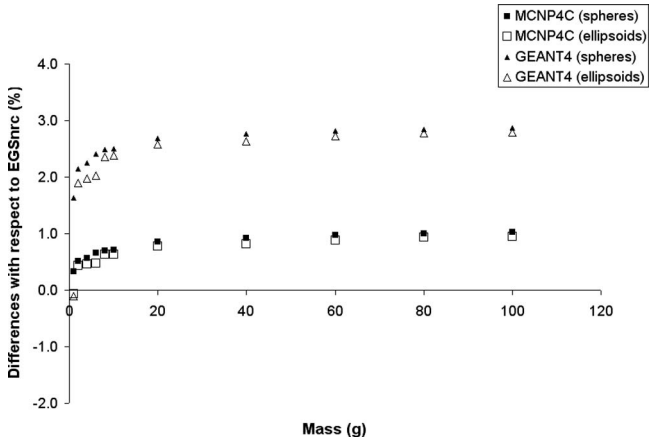

FIG. 13. Comparison of absorbed dose calculation for unit of cumulated activity, among several MC codes, for ^{188}Re. Calculations are referred to the *S*-value tabulations for the 3 mm voxel size. The data are reported in terms of the percent differences with respect to the calculations obtained by the EGSnrc voxel *S* values for both spherical and ellipsoidal masses.

these differences among the MC codes can affect considerably dose depositions at small distances, leading to noteworthy variations (about 9% for ^{131}I) when considering the convolution calculation of the absorbed dose.

In conclusion, when dose estimations with voxelized *S* formalism are performed, variations among different MC codes are expected to be within a few percent. For radionuclides where low-energy electrons cover an important part of the emission spectrum, more consistent differences may be obtained if older MC codes are employed.

[a]Author to whom correspondence should be addressed. Electronic mail: mpacilio@scamilloforlanini.rm.it

[1]R. W. Howell, B. W. Wessels, and R. Loevinger, "The MIRD perspective 1999," J. Nucl. Med. **40**, 3S–10S (1999).
[2]J. A. Siegel *et al.*, "MIRD Pamphlet No. 16: Techniques for quantitative radiopharmaceutical biodistribution data and analysis for use in human radiation dose estimates," J. Nucl. Med. **40**, 37S–61S (1999).
[3]W. E. Bolch *et al.*, "MIRD Pamphlet No. 17: The dosimetry of nonuniform activity distributions—Radionuclide *S* values at the voxel level," J. Nucl. Med. **40**, 11S–36S (1999).
[4]A. Dieudonné, W. Bolch, and I. Gardin, "3D internal dosimetry for radioimmunotherapy using voxel *S*-values approach," J. Nucl. Med. **48**, 298P (2007).
[5]I. Kawrakow, M. Fippel, and K. Friedrich, "3D electron dose calculation using a voxel based Monte Carlo algorithm (VMC)," Med. Phys. **23**, 445–457 (1996).
[6]J. Gardner, J. Siebers, and I. Kawrakow, "Dose calculation validation of YMC++ for photon beams," Med. Phys. **34**, 1809–1818 (2007).
[7]R. E. P. Taylor, G. Yegin, and D. W. O. Rogers, "Benchmarking BrachyDose: Voxel based EGSnrc Monte Carlo calculations of TG-43 dosimetry parameters," Med. Phys. **34**, 445–457 (2007).
[8]P. Edimo, C. Clermont, M. G. Kwato, and S. Vynckier, "Evaluation of a commercial YMC++ Monte Carlo based treatment planning system for electron beams using EGSnrc/BEAMnrc simulations and measurements," Phys. Med. (to be published).
[9]R. Wang and X. Allen Li, "Monte Carlo dose calculations of beta-emitting sources for intravascular brachytherapy: A comparison between EGS4, EGSnrc, and MCNP," Med. Phys. **28**, 134–141 (2001).
[10]O. Chibani and X. Allen Li, "Monte Carlo dose calculations in homogeneous media and at interfaces: A comparison between GEPTS, EGSnrc, MCNP, and measurements," Med. Phys. **29**, 835–847 (2002).
[11]L. Strigari, E. Menghi, M. D'Andrea, and M. Benassi, "Monte Carlo dose voxel kernel calculations of beta-emitting and Auger-emitting radionuclides for internal dosimetry: A comparison between EGSnrcMP and EGS4," Med. Phys. **33**, 3383–3389 (2006).
[12]M. Cristy and K. F. Eckerman, "Specific absorbed fractions of energy at various ages from internal photon sources," Oak Ridge National Laboratory Report No. ORNL/TM-8381/V1, 1987 (unpublished).
[13]"MCNP4C—a general Monte Carlo n-particle transport code, version 4c," Los Alamos National Laboratory Report No. LA-13709-M, 2000 (unpublished).
[14]F. Mourtada, C. G. Soares, S. M. Seltzer, P. M. Bergstrom, Jr., J. M. Fernández-Verea, J. Asenjo, and S. H. Lott, "Dosimetry characterization of a ^{32}P source wire used for intravascular brachytherapy with automated stepping," Med. Phys. **30**, 959–971 (2003).
[15]I. Kawrakow, "Accurate condensed history Monte Carlo simulation of electron transport. I. EGSnrc, the new EGS4 version," Med. Phys. **27**, 485–498 (2000).
[16]B. Walters, I. Kawrakow, and W. O. D. Rogers, "DOSXYZnrc users manual," National Research Council of Canada Technical Report No. PIRS-794, 2005 (unpublished).
[17]S. Agostinelli *et al.*, "Geant4: A simulation toolkit," Nucl. Instrum. Methods Phys. Res. A **506**, 250–303 (2003).
[18]E. Poon and F. Verhaegen, "Accuracy of the photon and electron physics in GEANT4 for radiotherapy applications," Med. Phys. **32**, 1696–1711 (2005).
[19]J. A. Halbleib, R. P. Kensek, G. D. Valdez, S. M. Seltzer, and M. J. Berger, "ITS Version 3.0: Integrated TIGER series of coupled electron/photon Monte Carlo transport codes," IEEE Trans. Nucl. Sci. **39**, 1025–

1030 (1992).
[20]N. Jabbari, B. Hasemi-Malayeri, A. R. Farajollahi, A. Kazemnejad, A. Shafaei, and S. Jabbari, "Comparison of MCNP4C and EGSnrc Monte Carlo codes in depth-dose calculation of low energy clinical electron beams," J. Phys. D **40**, 4519–4524 (2007).
[21]M. Cremonesi, M. Ferrari, C. M. Grana, A. Vanazzi, M. Stabin, M. Bartolomei, S. Papi, G. Prisco, G. Martinelli, G. Paganelli, and P. F. Ferrucci, "High-dose radioimmumotherapy with ^{90}Y-Ibritumomab Tiuxetan: Comparative dosimetric study for tailored treatment," J. Nucl. Med. **48**, 1871–1879 (2007).
[22]C. Chiesa, F. Botta, E. Di Betta, A. Coliva, M. Maccauro, G. Aliberti, S. Bavosi, L. Devizzi, A. Guidetti, E. Seregni, A. M. Gianni, and E. Bombardieri, "Dosimetry in myeloablative ^{90}Y-labeled Ibritumomab Tiuxetan therapy: Possibility of increasing administered activity on the base of biological effective dose evaluation. Preliminary results," Cancer Biother. Radiopharm. **22**, 113–120 (2007).
[23]M. G. Stabin, "Uncertainties in internal dose calculations for radiopharmaceuticals," J. Nucl. Med. **49**, 853–860 (2008).